Band formation and defects in a finite periodic quantum potential

(Dated: May 20, 2021)

Abstract

Periodic quantum systems often exhibit energy spectra with well-defined energy bands separated by band gaps. The formation of band structure in periodic quantum systems is usually presented in the context of Bloch's theorem or through other specialized techniques. Here we present a simple model of a finite one-dimensional periodic quantum system that can be used to explore the formation of band structure in a straightforward way. Our model consists of an infinite square well containing several evenly-spaced identical Dirac delta wells. Both attractive and repulsive delta wells are considered. We solve for the energy eigenvalues and eigenfunctions of this system directly and show the formation of band structure as the number of delta wells is increased, as well as how the size of the bands and gaps depends on the strength of the delta wells. These results are compared ot the predictions from Bloch's theorem. In addition, we use this model to investigate how the energy spectrum is altered by the introduction of two types of defects in the periodicity of the system. Strength defects, in which the strength of one delta well is changed, can result in an energy level moving from one band, through the band gap, to another band as the strength of the well is varied. Position defects, in which the location of one delta well is changed, can modulate the size of the energy bands and sufficiently large position defects can move an energy level into a gap. Band structure and defects are important concepts for understanding many properties of quantum solids and this simple model provides an elementary introduction to these ideas.

I. INTRODUCTION

In a crystalline solid, individual atoms are brought together in a regular arrangement. We can imagine constructing a one-dimensional crystal by starting with a single atom and then successively adding more and more identical atoms, equally spaced along a line. While isolated, each of these atoms has the same set of bound state energy eigenvalues. However, as the second atom is brought closer to the first each level of the isolated atom will split into two distinct levels in the combined system of two closely spaced atoms, with the amount of splitting depending on the interatomic separation. For a system of N closely spaced atoms, each isolated level splits into N distinct levels. As N becomes very large the split levels form a practically continuous band of energy eigenvalues.[1] Each band is typically separated from adjacent bands by a noticeable gap. This process is sometimes called the level splitting route to band formation. Level splitting and band structure can also occur in acoustical systems and systems of coupled classical oscillators.[2–4]

Energy bands and band gaps play an important role in determining properties of a solid such as its electrical conductivity. In insulators the highest-energy levels occupied by electrons in the ground state of the solid completely fill one band (the valence band) which is separated by a large gap from the band containing the lowest-energy levels that are unoccupied in the ground state (the conduction band). Thermal excitations cannot excite electrons from the valence band into the conduction band and these materials do not conduct electricity. Semiconductors have a small gap between the valence and conduction bands, so electrons can be thermally (or otherwise) excited into the conduction band. In metals there is no gap between the highest occupied levels and the lowest unoccupied levels (for example, if a band is only partially filled when the solid is in its ground state), so electrons can easily be excited to higher levels and these materials conduct electricity quite well.

A detailed understanding of the formation of band structure can be gained by investigating quantum mechanical systems with spatially periodic potential energy functions. Students are typically introduced to these models in the context of Bloch's theorem.[5,6] Bloch's theorem provides a method for determining the band structure of a perfectly periodic quantum system using only knowledge about the potential energy in a single unit cell. A classic example of the application of Bloch's theorem is the derivation of band structure in the Kronig-Penney model, which consists of periodic rectangular barriers.[7] However, Bloch's

theorem is somewhat abstract and it may be difficult for novice quantum mechanics students to understand. Other methods for deriving the band structure of a perfectly periodic quantum system may be similarly challenging.[8,9]

Another aspect of Bloch's theorem that may be confusing for novice students is that it only applies exactly to infinite periodic systems. A finite system has boundaries, or surfaces, that necessarily disrupt the periodicity. Several methods have been presented for computing energy eigenvalues in finite periodic systems to illustrate level splitting and the formation of band structure,[10–12] but these methods involve analytical techniques or numerical methods that may be unfamiliar to students. Other studies examine transmission resonances in the scattering of particles passing through finite periodic potentials.[13–19] These scattering studies show energy ranges for the incident particle that give rise to near-perfect transmission while other energy ranges produce almost no transmission. These transmission bands are closely related to the energy bands for the periodic potential.[20] Some of these scattering studies use fairly elementary methods, but they do not directly show the formation of band structure in the energy spectrum.

Another problem with the methods mentioned above is that they do not allow for the investigation of defects in the periodic system. A defect is simply a disruption of the periodicity in the (finite or infinite) potential energy function of the system. Although the boundaries of a finite periodic system represent one type of defect, many other types of defects exist in real solids. For example, an atom in the solid may be displaced from its usual location (Frenkel defect) or it may be missing altogether (vacancy defect). Another important example is a substitutional defect or impurity defect, when an atom in the perfect solid is replaced with a different atom. Defects can play an important role in determining the properties of a solid. In fact, the doping of semiconductors to alter their properties involves the intentional introduction of impurities into the semiconductor crystal. Some prior studies have investigated impurity-type defects in simple one-dimensional systems, but these studies make use of numerical methods that are likely unfamiliar to students.[21,22]

In this paper we present a very simple model for investigating the level-splitting route to band formation in a finite periodic quantum potential built from two potentials widely-used for quantum mechanics pedagogy: the infinite square well and Dirac delta wells.[23] In Section II we present the infinite version of this model without the square well and discuss the results of Bloch's theorem. In Section III we add the square well to impose boundaries

and show how the energy eigenvalues of the resulting finite system can be found using elementary methods. Then, in Section IV, we show that this model exhibits level splitting as the number of delta wells is increased and we investigate how the size of the energy bands depends on the strength of the delta wells. A similar approach was taken in Ref. 24, but that study employs delta barriers rather than delta wells. The use of delta wells gives rise to negative-energy (and sometimes even zero-energy) eigenstates that may give a more realistic picture of the behavior of quantum solids.[25] Finally, in Section V, we use this simple model to investigate two types of defects: strengths defects which are similar to impurities, and position defects which are similar to Frenkel defects. Computer code for carrying out these investigations is provided, as described in Section VI.

II. INFINITE PERIODIC MODEL

The model we will examine consists of a sequence of Dirac delta wells. The potential energy function for each delta well is

$$V_i(q) = -\alpha_i \delta(q - d_i), \tag{1}$$

where α_i is the "strength" or "intensity" of each well and d_i specifies the location of each well. The d_i are always assumed to be well-ordered such that $d_{i+1} > d_i$ for all i. The truly periodic version of our model consists of an infinite number of these delta wells, each with identical strength $\alpha_i = \alpha$, and with $d_i = ia$ for some uniform spacing a. In what follows we will continue to use d_i, α_i, etc. so that we can easily adapt our model to include boundaries and defects.

We want to find the energy eigenvalues ε and eigenfunctions $\phi(q)$ of this system. The eigenfunctions must satisfy the energy eigenvalue equation (also called the time-independent Schrödinger equation, or TISE):

$$-\frac{\hbar^2}{2m}\frac{d^2}{dq^2}\phi(q) + \sum_i V_i(q)\phi(q) = \varepsilon\phi(q). \tag{2}$$

To make our model dimensionless we introduce the dimensionless coordinate $x = q/a$. We also define $b_i = d_i/a$, so for our periodic model $b_i = i$. We can rewrite Eq. 1 in terms of these dimensionless quantities:

$$V_i(ax) = -\frac{\alpha_i}{a}\delta(x - b_i), \tag{3}$$

where we have made use of the identity $\delta(ax) = \delta(x)/|a|$.

The TISE (Eq. 2) for our scaled model becomes

$$-\frac{\hbar^2}{2ma^2}\frac{d^2}{dx^2}\psi(x) - \frac{1}{a}\sum_i \alpha_i \delta(x - b_i)\psi(x) = \varepsilon\psi(x) \tag{4}$$

where $\psi(x) = \sqrt{a}\phi(ax)$ is a dimensionless wave function. We can rewrite Eq. 4 as

$$\frac{d^2}{dx^2}\psi(x) + \sum_i \beta_i \delta(x - b_i)\psi(x) = -E\psi(x), \tag{5}$$

where $\beta_i = 2ma\alpha_i/\hbar^2$ is the scaled well strength and $E = 2ma^2\varepsilon/\hbar^2$ is the scaled energy eigenvalue (both of which are dimensionless).

To solve for the eigenvalues and eigenfunctions we first break up $\psi(x)$ into pieces divided by the locations of the delta wells. Each piece $\psi_j(x)$ is defined on the subinterval $b_j < x < b_{j+1}$. Within each subinterval Eq. 5 reduces to

$$\frac{d^2}{dx^2}\psi_j(x) = -E\psi(x). \tag{6}$$

If $E > 0$ then the solution to Eq. 6 can be written as

$$\psi_j^+(x) = A_j^+ \sin\left(k(x - b_j)\right) + B_j^+ \cos\left(k(x - b_j)\right), \tag{7}$$

where $E = k^2$. If $E < 0$ then the solution to Eq. 6 can be written as

$$\psi_j^-(x) = A_j^- e^{-\kappa(x-b_j)} + B_j^- e^{\kappa(x-b_j)}, \tag{8}$$

where $E = -\kappa^2$.

We require that $\psi(x)$ be continuous everywhere. Continuity at the locations of the delta wells implies that

$$\psi_{i-1}(b_i) = \psi_i(b_i). \tag{9}$$

At the locations of the delta wells $d\psi/dx$ is discontinuous, but the discontinuity must satisfy the condition[26]

$$\lim_{\epsilon\to 0}\left(\left.\frac{d\psi}{dx}\right|_{x=b_i+\epsilon} - \left.\frac{d\psi}{dx}\right|_{x=b_i-\epsilon}\right) = -\beta_i \lim_{\epsilon\to 0}\int_{b_i-\epsilon}^{b_i+\epsilon}\delta(x - b_i)\psi(x)dx, \tag{10}$$

or

$$\left.\frac{d\psi_i}{dx}\right|_{x=b_i} - \left.\frac{d\psi_{i-1}}{dx}\right|_{x=b_i} = -\beta_i\psi_i(b_i). \tag{11}$$

Bloch's theorem states that the energy eigenfunctions for the infinite periodic system satisfy $\psi(x+1) = e^{iK}\psi(x)$.[5] From this condition, with the general solution given in Eq. 7 and the conditions given by Eqs. 9 and 11, one can show that the positive energy eigenvalues are given by $E = k^2$ where k is a solution to

$$\cos(K) = \cos(k) - \frac{\beta}{2k}\sin(k). \tag{12}$$

Since K can have any real value, the left side of Equation 12 can take on any value between -1 and 1. Thus, values of k such that the right side of Eq. 12 is between -1 and 1 give valid solutions (within the "Bloch band"), while values of k for which this condition does not hold are not valid solutions (outside of the Bloch band, thus forming a gap). The limits of the Bloch bands can be determined by finding the values of k that make the right side of Eq. 12 exactly equal to ± 1. Note that $k = n\pi$ makes the right side of Eq. 12 equal 1 for any integer n.

We also can apply Bloch's theorem to the negative energy states of the infinitely periodic version of this system, this time using Eq. 8 along with the conditions given by Eqs. 9 and 11. The resulting energies are given by $E = -\kappa^2$ where

$$\cos(K) = \cosh(\kappa) - \frac{\beta}{2\kappa}\sinh(\kappa). \tag{13}$$

Again, the limits of the (single) Bloch band are found when the right side of Eq. 13 is equal to ± 1.

III. FINITE PERIODIC MODEL

In the finite version of our model we include only a finite number of delta wells, located at $b_i = i$ for $i = 1, 2, \ldots, N$. We then impose hard boundaries at $x = b_0 = 0$ and $x = b_{N+1} = N + 1$, effectively embedding our system of delta wells inside an infinite square well of width $N + 1$ in our scaled distance units. Note that the spacing between the outermost delta wells and the hard walls is equal to the spacing between the delta wells. Thus, the hard walls impose a boundary (or surface) that makes the system finite but in such a way as to minimize the disruption of the system's periodicity. The wave functions will be divided into $N + 1$ pieces, psi_i, with $i = 0, 1, \ldots, N$. At the boundaries the wave function must go to zero, so we have

$$\psi_0(0) = 0 \tag{14}$$

and

$$\psi_N(N+1) = 0. \tag{15}$$

Our finite model is no longer periodic, due to the boundaries. Therefore, we cannot use Bloch's theorem and must instead employ more direct methods for determining our energy eigenvalues and eigenfunctions. For $E > 0$ our eigenfunction still takes the form given in Eq. 7. Using this solution, Eq. 14 gives $B_0^+ = 0$. Since we are not worried about obtaining normalized eigenfunctions we will simply let $A_0^+ = 1$. Eqs. 9 and 11 then give a system of equations whose solution can be written in matrix form as

$$\begin{pmatrix} A_i^+ \\ B_i^+ \end{pmatrix} = \mathbf{T}_{i,i-1}^+ \begin{pmatrix} A_{i-1}^+ \\ B_{i-1}^+ \end{pmatrix}, \tag{16}$$

where

$$\mathbf{T}_{i,i-1}^+ = \begin{pmatrix} c_i - \frac{\beta_i}{k} s_i & -s_i - \frac{\beta_i}{k} c_i \\ s_i & c_i \end{pmatrix}, \tag{17}$$

and $c_i = \cos\left(k(b_i - b_{i-1})\right)$ while $s_i = \sin\left(k(b_i - b_{i-1})\right)$. The matrix $\mathbf{T}^+$ is known as a transfer matrix.[27] Note that the Bloch equation (Eq. 12) for the infinite periodic system can be derived by simply setting $\cos(K) = \mathrm{Tr}(\mathbf{T}^+)/2$.

We can then determine the coefficients for any portion of the energy eigenfunction using

$$\begin{pmatrix} A_n^+ \\ B_n^+ \end{pmatrix} = \prod_{i=1}^{n} \mathbf{T}_{i,i-1}^+ \begin{pmatrix} 1 \\ 0 \end{pmatrix}. \tag{18}$$

Equation 18 can be used to find A_N^+ and B_N^+ in terms of k. Eq. 15 then gives

$$A_N^+ \sin\left(k(N+1-b_N)\right) + B_N^+ \cos\left(k(N+1-b_N)\right) = 0. \tag{19}$$

Equation 19 is a transcendental equation that can be solved numerically using standard root-finding algorithms to find allowed values of k, of which there will be an infinite number.

Once a value of k that solves Eq. 19 has been determined we can then compute the scaled energy eigenvalue using $E = k^2$. The (unnormalized) energy eigenfunction is the piecewise function defined by Eq. 7 with values for A_n^+ and B_n^+, for $n = 1, \ldots, N$, found using Eq. 18.

The procedure is similar for finding solutions with $E < 0$ but now the eigenfunction takes the form given in Eq. 8. Using this solution, Eq. 14 gives $B_0^- = -A_0^-$. Since we are not

worried about obtaining normalized eigenfunctions we will simply let $A_0^- = 1$ and $B_0^- = -1$. The transfer matrix for the negative energy solutions is

$$\mathbf{T}_{i,i-1}^- = \begin{pmatrix} (1+\frac{\beta_i}{2k})e^{-\kappa(b_i-b_{i-1})} & \frac{\beta_i}{2k}e^{\kappa(b_i-b_{i-1})} \\ -\frac{\beta_i}{2k}e^{-\kappa(b_i-b_{i-1})} & (1-\frac{\beta_i}{2k})e^{\kappa(b_i-b_{i-1})} \end{pmatrix}. \tag{20}$$

The coefficients for the eigenfunction are given by

$$\begin{pmatrix} A_n^- \\ B_n^- \end{pmatrix} = \prod_{i=1}^{n} \mathbf{T}_{i,i-1}^- \begin{pmatrix} 1 \\ -1 \end{pmatrix}. \tag{21}$$

Equation 21 can be used to find A_N^- and B_N^- in terms of k. Eq. 15 then gives

$$A_N^- e^{-\kappa(N+1-b_N)} + B_N^- e^{\kappa(N+1-b_N)} = 0. \tag{22}$$

Equation 22 is again a transcendental equation that can be solved numerically to find allowed values of k, but this time there will be at most N solutions.

Once a value of k that solves Eq. 22 has been determined we can then compute the scaled energy eigenvalue using $E = -\kappa^2$. The (unnormalized) energy eigenfunction is the piecewise function defined by Eq. 8 with values for A_n^- and B_n^-, for $n = 1, \ldots, N$, found using Eq. 21.

In addition to positive and negative energy solutions, it is possible for this model to admit nontrivial energy eigenfunctions with zero energy.[28–31] A zero-energy eigenfunction will be a piecewise linear wave function given by

$$\psi_j^0(x) = A_j^0 + B_j^0(x - b_j). \tag{23}$$

Eq. 14 gives $A_0^0 = 0$, so to get unnormalized solutions we can simply set $B_0^0 = 1$. The transfer matrix for the zero-energy solution is

$$\mathbf{T}_{i,i-1}^0 = \begin{pmatrix} 1 & b_i - b_{i-1} \\ -\beta_i & 1 - \beta_i(b_i - b_{i-1}) \end{pmatrix}. \tag{24}$$

The coefficients for the eigenfunction are given by

$$\begin{pmatrix} A_n^0 \\ B_n^0 \end{pmatrix} = \prod_{i=1}^{n} \mathbf{T}_{i,i-1}^0 \begin{pmatrix} 0 \\ 1 \end{pmatrix}. \tag{25}$$

Equation 25 can be used to find A_N^0 and B_N^0. The value of the wave function at the right wall ($x = N + 1$) is then

$$\psi_N^0(N+1) = A_N^0 + B_N^0(N + 1 - b_N). \tag{26}$$

If $\psi(N+1) = 0$ then the system admits a zero-energy eigenfunction given by Eq. 23. If $\psi(N+1) \neq 0$ then the system does not admit a zero-energy eigenfunction (other than the trivial solution $\psi(x) = 0$). There can be *at most* one nontrivial zero-energy eigenfunction in our model with a given set of parameters.

IV. LEVEL SPLITTING AND BAND FORMATION

A. Increasing the number of delta wells

We begin our investigation of the finite periodic model by exploring the phenomenon of level splitting. Level splitting occurs when a perturbation to a system causes two previously identical (degenerate) energy levels to split into distinct levels. Level splitting can occur when two quantum subsystems with identical energy levels are allowed to interact with each other. The interaction breaks the degeneracy in the energy eigenvalues and as a result the combined system will have two different energy eigenvalues in place of the single eigenvalue that existed in each subsystem without interaction. In effect, a single energy level is split into two levels as a result of the interaction between the subsystems. The separation between the two split levels will generally depend on the strength of the interaction between the two subsystems.

In our simple model, level splitting occurs as we increase the number of delta wells N in the system. The hard walls and the delta wells are periodically spaced so that $b_i = i$. Thus, as we add more delta wells we are also increasing the width of the infinite square well which is always $N+1$. The spaces between the hard walls and the delta wells, or between adjacent delta wells, can be viewed as quantum subsystems. If these segments did not interact then each would constitute an infinite square well of width a with scaled energy eigenvalues given by

$$E_j^{ISW} = \pi^2 j^2. \tag{27}$$

The delta wells, however, are not hard walls. They permit coupling between these quantum subsystems and the strength of that coupling is determined by the strength of the delta well. Smaller values of β lead to stronger coupling and as $\beta \to 0$ the system just becomes an infinite square well of width $N+1$. As $\beta \to \pm\infty$ the coupling between the subsystems vanishes and the full system degenerates into a collection of $N+1$ infinite square wells each

with unit width.[32]

To illustrate level splitting in our simple model we will examine the energy eigenvalues of the system for finite β as we increase the number of evenly spaced delta wells N. We choose $\beta_i = 10$ for all of the delta wells. Figure 1 shows the $4N + 4$ lowest energy eigenvalues for the system as N increases from 0 to 9.

For $N = 0$ the energies are just the eigenvalues for the ISW with unit width, as expected. The introduction of a delta well for $N = 1$ creates a new energy level close to, but separate from, each of the levels for $N = 0$, thus illustrating level splitting. In addition, at $N = 1$ we see that the system supports a negative energy state at $E \approx -\beta^2/4$, which is the energy of a bound state for a single, isolated delta well.[33] For $N = 2$ we see that each ISW level has split into three levels that are close to each other but separated from the groups associated with different ISW states. Likewise, the negative energy level from $N = 1$ has split into two closely-spaced levels, as can be seen in Figure 2 which shows a detail of the negative energy levels from Fig. 1. For $\beta = 10$ this model does not support zero-energy states for any value of N.

Note that for this system the energy eigenvalues for the unit-width ISW (Eq. 27) are always eigenvalues for the system, regardless of the value of N.[34] The eigenfunctions associated with these energies are sinusoidal functions that go to zero at the hard walls and at the location of each delta well, thus these eigenfunctions do not "see" the delta wells at all and are not affected by their presence or absence. The eigenfunctions for the other levels in each group do not have this property and thus the other eigenvalues do change as N changes.

As N is increased further we see that each ISW level splits into a group of $N + 1$ levels, while the negative energy levels form a group of N levels. Each group of eigenvalues spans a limited range of energy. For $E > 0$ the energy of the ISW state sets the lower limit for this range, while the upper limit increases with N. However, Fig. 1 shows that the upper limit approaches a limiting value as N becomes very large. The energy range spanned by a group of levels associated with a particular ISW state can be thought of as an "energy band" and there are noticeable "gaps" between the bands. In the limit $N \to \infty$ each band would define a practically continuous range of energy eigenvalues for the system, but the gaps between the bands would persist showing that even in the limit of an infinite number of delta wells there are some energies that are not permitted.

The width of each energy band is approximately equal to twice the separation between

the two levels in that band for $N = 1$. In fact, if we ignore the ISW state, the pattern of energy levels for $N \geq 1$ appears to be nearly symmetric around the new level that appears at $N = 1$, although this symmetry is somewhat distorted by the presence of the ISW state which forms a lower bound for the energy band. Thus, by solving the system with a single delta well we can get a good estimate for the location and size of each energy band for the case with an arbitrary number of delta wells.

Note that the widths of the bands increase as energy increases, and thus the band gaps are smaller at higher energies. We have already noted that the coupling between subintervals that leads to level splitting depends on the value of β, with larger values of β producing smaller coupling and thus smaller bands (and larger gaps). However, the coupling between subintervals also depends on the particle's energy. At higher energies the coupling will be stronger because a high-energy particle can more easily pass from one subinterval to another. In terms of scattering, the transmission coefficient for a particle to be transmitted across a delta well is closer to one when the particle has higher energy.[35] This stronger coupling between subintervals leads to wider bands and narrower gaps at higher energies.

For comparison in Figure 1 we show the limits of the bands derived from Bloch's theorem (see Section II). In Fig. 1 we see that the ISW states lie at the bottom of each positive-energy band, in perfect agreement with the results from Bloch's theorem. The ISW states are eigenstates of the infinite system and they remain so for the finite system because we have effectively replaced two delta wells in the infinite system with hard walls, but the ISW states already have nodes at those locations so they remain unchanged. In contrast, we see that the highest-energy state in each band fails to reach the upper limit of the Bloch band. Thus we see that the transition from an infinite periodic system to a finite one, as a result of introducing the infinite square well boundaries, leads not only to a finite number of states in each band but also a slight decrease in the upper limit of each band.

The negative energy levels are also confined to a band of finite width, but in this case the band is quite narrow with all of the states close to the bound state energy for a single isolated delta well, as shown in Figure 2. There is an intuitive reason for the rather minimal level splitting for the negative energies. Bound state wave functions for a delta well are exponentially localized near the location of the well, so as two wells are brought together there will be minimal overlap of these wave functions and thus only weak coupling and small level splitting. Like the positive energy bands, the negative energy band is nearly symmetric

around the level that appears at $N = 1$. The Bloch limits for the negative energy states are shown in Figs. 1 and 2. It is clear that the negative energy eigenvalues lie within a band that is somewhat narrower than the Bloch band, but which approaches the limits of the Bloch band as N is increased.

B. Changing delta well strength

In the previous section we explored how increasing the number of delta wells led to the formation of energy bands separated by band gaps in the eigenvalue spectrum. Now we will explore how changing the strength of the delta wells affects the eigenvalue spectrum. Figure 3 shows the 40 lowest energy eigenvalues as a function of β for our model system with $N = 9$ evenly spaced delta wells each with strength β. The data for $\beta = 10$ in Fig. 3 corresponds to the data for $N = 9$ in Fig. 1.

Note that Fig. 3 displays four horizontal lines: these are the unit-width ISW eigenvalues (Eq. 27) for $j = 1$ to 4. The corresponding eigenfunctions all go to zero at the locations of the delta wells, so they are unaffected by changes in β. However, the eigenvalues for all other states move toward lower energies as β is increased and toward higher energies as β is decreased. This makes sense given the definition of the potential in Eq. 1. In a one-dimensional system like our model there can be no degeneracies (two different eigenstates with the same eigenvalue), so it is impossible for the eigenvalue curves in Fig. 3 to cross each other. As a result, for large positive β the eigenvalues push downward into the ISW states, forming compact energy bands with the ISW states as the lower bound and large gaps between the bands. Similarly, for large negative β (such that the delta "wells" become "barriers") the non-ISW eigenvalues push upward to form compact bands with the ISW states as the upper bound and large gaps between the bands. In the limit $\beta \to \pm\infty$ the positive energy states will all become degenerate with the ISW states as the system becomes a set of $N + 1$ uncoupled ISWs with unit width and the Pauli exclusion principle no longer prohibits this "coexistence degeneracy."[32] When $\beta = 0$ the eigenvalues are just those for an infinite square well with width $N + 1$ and there are no bands or gaps.

Note that there is no ISW state with negative energy, so for positive β there is no lower bound to halt the movement of the negative energy eigenvalues. Instead, these eigenvalues continue to decrease as β is increased. In fact, these negative energy eigenvalues will cluster

around $E = -\beta^2/4$, which is the energy of the bound state for a single isolated delta well with strength β. As β increases, the cluster becomes more compact and for large values of β the eigenvalues are nearly (but not actually) degenerate. For small values of β the cluster is more spread out and for sufficiently small positive values of β some of the states in this cluster will have positive energies. For $\beta = 2$ one of these states has $E = 0$. Although it is not obvious from Fig. 3, all of the states have $E > 0$ for $\beta < \epsilon$ where ϵ is a small positive number. This result illustrates the fact that, although an isolated delta well always supports a bound state for any $\beta > 0$, a delta well placed inside an infinite square well may not support a bound state if β is small or if the boundaries are close to the delta well.

Fig. 3 also shows the limits of the Bloch bands as a function of β. All of the energy eigenvalues for the model with $N = 9$ lie within the Bloch bands, with the unit-width ISW states lying exactly on the lower (for $\beta > 0$) or upper (for $\beta < 0$) boundary of the positive-energy bands.

C. Properties of eigenfunctions

Figure 4 shows some examples of (unnormalized) energy eigenfunctions for this system with $N = 9$ and various values of β. The index n indicates the number of the eigenfunction ordered by energy with the lowest (negative) energy state as $n = 1$. For $\beta = 1$ (top row) all three states have positive energy eigenvalues. For $\beta = 2$ (middle row) the $n = 4$ state has a negative energy, while $n = 5$ is a zero-energy state and $n = 6$ has a positive energy. For $\beta = 3$ (bottom row) all three states have negative energies. With these examples it is not hard to visualize how each eigenstate changes from sinusoidal (positive energy) to linear (zero energy) to exponential (negative energy) while retaining a similar overall shape as β is increased.

As expected from Eqns. 7, 8, and 23 the positive energy states are sinusoidal, the negative energy states are exponential, and the zero-energy state is linear in the regions between the walls and delta wells. All wave functions are continuous, but in general there are discontinuities in the first derivative of each wave function at the location of each delta well, with larger values of β generally producing greater discontinuities. An exception to this general rule is when the wave function has a node (where $\psi(x) = 0$) at the location of a delta well. In that case, there is no discontinuity in $d\psi/dx$ because, by Eq. 11, the

discontinuity is proportional to both β_i and $\psi(b_i)$. Therefore, when $\psi(b_i) = 0$ there is no "cusp" or "corner" at that location and the wave function passes smoothly over the axis at that point. Several examples of this phenomenon are visible in Fig. 4, such as the $n = 5$ state at all even values of x.

Because the potential energy function is symmetric about the center of the well ($x = 5$ for the 9 well case), the energy eigenfunctions will have a definite even or odd symmetry. As seen in Fig. 4, the odd-numbered states have even symmetry while the even-numbered states have odd symmetry.

One final thing to note about the eigenfunctions for this model is that the eigenfunction for the n^{th} state will have $n - 1$ nodes (not counting the nodes at the walls of the ISW). It is easy to identify the state number of an eigenfunction by simply counting the nodes and adding one.

V. EXPLORING DEFECTS

In the previous section we examined the effects of changing the strength of *all* of the delta wells in our model. Now we will investigate what happens if we change the parameters of only a single delta well, while leaving all other wells unchanged. If we change one of the delta wells without making corresponding changes to the other wells we disrupt the periodicity of the system. Such a disruption of periodicity is known as a *defect*. Defects result in alterations to the energy spectrum of the system. In particular, defects can lead to the appearance of energy levels within the band gaps of the fully periodic system. This modification of the band gaps can have important consequences for the electrical, optical, or structural properties of real physical systems like semiconductor crystals. The so-called "doping" of semiconductors is the intentional introduction of impurities to create defects in the crystal lattice and thus alter the properties of the crystal.

Our simple one-dimensional model admits point defects, but not line or surface defects which can only exist in higher dimensions. We investigate two types of point defects in our model system: strength defects and position defects. A strength defect is one in which the strength β_i of one of the delta wells differs from the strength of the other wells. These strength defects are similar to impurity defects in real crystals, in which one of the atoms in the crystal is replaced with a different type of atom. If the strength of the defect well is

set to zero then the strength defect can also be used to model a vacancy in which one of the lattice sites in the crystal is unoccupied. A position defect is one in which the position b_i of one of the delta wells deviates from the even spacing maintained by the other wells. Position defects are comparable to Frenkel defects in real crystals, in which one of the atoms in the crystal is displaced from its normal location. We will now investigate how both types of defect alter the energy spectrum and the structure of the eigenfunctions in this system.

A. Strength defects

To investigate a strength defect we leave the delta wells at their usual positions and give each one a scaled strength β, except that we choose to modify the strength of one of the wells. Figure 5 shows the results for a strength defect located at the seventh of nine evenly spaced wells.[36] The plot shows the energy eigenvalues as a function of the defect well strength β_7. All other wells have scaled strength $\beta = 10$, so the results for $\beta_7 = 10$ correspond exactly to the results for $\beta = 10$ in Fig. 3 as well as for $N = 9$ in Fig. 1. The Bloch bands for the infinitely periodic system with $\beta = 10$ are shown in Fig. 5 for reference.

Examination of Fig. 5 shows that the strength defect has a significant effect on the eigenvalue spectrum. However, it does not have an equally dramatic effect on each eigenvalue. Some eigenvalues change very little as β_7 is varied while others change considerably. For positive energy states the general pattern is that as β_7 is decreased from 10 the highest level in a particular band moves into the band gap and eventually approaches the ISW level at the bottom of the next higher band for large negative values of β_7. Meanwhile the highest of the negative energy levels moves upward, eventually becoming positive and approaching the ISW value at the bottom of the first positive band for large negative values of β_7. The remaining negative energy states remain tightly clustered near $E = -25$. Note that for $\beta_7 = 0$, which corresponds to a vacancy at the seventh lattice site, the top levels of the two lowest positive energy bands have moved well into the band gap and one of the negative energy states has moved up into the gap below the first positive energy band.

The movement of an energy level into and through a band gap is closely related to what happens when semiconductor crystals are doped by the introduction of impurities into the crystal lattice. The introduction of dopant atoms into the crystal generates a defect in the doped crystal structure and can lead to energy levels that appear within the band gap of

the pure semiconductor crystal. If the dopant is an electron donor then the energy level in the gap will be close to the (higher energy) conduction band and the material is known as an n-type semiconductor. If the dopant is an electron acceptor the energy level in the gap will be close to the (lower energy) valence band and the material is known as a p-type semiconductor. Many semiconductors devices involve junctions between p-type and n-type materials. In our simple model we can see that changing the value of β_7 can transform our system from a having a spectrum like that of a p-type material to having a spectrum like that of an n-type material.

If instead β_7 is increased from 10, the highest level in each positive energy band moves downward while the bottom state of each band is the ISW state that is not affected by changes to β_7. Thus, as β_7 increases the size of each band gradually decreases. The lowest of the negative energy states moves downward, approximately following the curve $E = -\beta_7^2/4$, which is the energy of the bound state for an isolated delta well with scaled strength β_7. Again, the other negative energy states remain clustered near $E = -25$ (the energy of an isolated delta well with strength $\beta = 10$). As $\beta_7 \to \pm\infty$ the system becomes divided into two separate ISWs, one of width 7 containing six delta wells and the other of width 3 containing two delta wells. The energy spectrum as $\beta_7 \to \pm\infty$ is therefore a mixture of the energy levels for a width-7 ISW and a width-3 ISW, although note that the eigenvalue for $\beta_7 \to -\infty$ is *not* adiabatically connected to the same eigenvalue for $\beta \to \infty$.

Figure 6 shows a detail from Fig. 5 to illustrate the behavior of the negative energy levels near $\beta_7 = 10$. The figure shows that the lowest eight energy eigenvalue curves are roughly horizontal for $\beta_7 < 9.9$ with values approximately equal to a mixture of the $N = 2$ and $N = 6$ results in Fig. 2. As β_7 is increased these curves are approached from above by the $n = 9$ curve and undergo a series of avoided crossings that push most of the states toward slightly lower energies. For $\beta_7 > 10.1$ the $n = 1$ curve slopes steeply downward while the curves for $n = 2$ to 9 are nearly horizontal again. In effect, the $n = 9$ curve transfers its behavior to the $n = 1$ curve while the other curves simply swap places.

Figure 7 shows selected (unnormalized) energy eigenfunctions for our model system with a strength defect at the seventh well. The $n = 9$ state is strongly peaked at the location of the defect ($x = 7$). This behavior is typical for a negative energy state that has moved out of the cluster of energies near $E = -25$. In contrast, the negative energy states that remain within that cluster have wave functions with probabilities concentrated on one side

of the defect or the other, as seen in the $n = 8$ state in Fig. 7. This result makes sense because in the limit $\beta_7 \to \pm\infty$ these states will become eigenstates of either a width-7 ISW with 6 delta wells on the left or a width-3 ISW with 2 delta wells on the right. The wave function for a positive energy state that has moved into a band gap, such as $n = 19$ in Fig. 7, will also be peaked at the location of the defect, but the effect is not as strong as for the negative energy state. The positive energy states that remain within an energy band show only a weak concentration of probability to one side or the other of the defect, as seen in the $n = 18$ state in Fig. 7, although this concentration becomes more pronounced as β_7 gets larger (except for the unit-width ISW state which is unaffected by β_7). It is no surprise that states with wave functions peaked at the location of the defect will have energy eigenvalues that change significantly as β_7 is changed.

The behavior shown for a strength defect at the seventh well is typical. Introducing a strength defect at a different well location produces qualitatively similar results, with one slight exception. If the defect is introduced at the fifth well, which lies at the exact center of the ISW, then the potential energy function is still symmetric about that center. Therefore, the energy eigenfunctions will retain their well-defined symmetry. The even-numbered states (which have odd symmetry) will be entirely unaffected by the defect. Odd symmetry states must have a node at $x = 5$, so these states don't "see" the defect. Even symmetry (odd-numbered) states, however, will be altered by the defect, and the defect can cause some energy levels to move out of their usual bands and into a band gap. The eigenfunctions associated with such levels will be peaked at $x = 5$. Note, however, that eigenfunctions associated with levels that remain in the cluster near $E = -25$ will no longer be concentrated on one side of the defect or the other, since they must retain their overall even or odd symmetry.

B. Position defects

To investigate a position defect we give all of the delta wells a common strength β and space the wells evenly, except that one well is displaced from its usual location. Figure 8 shows the results for a position defect located at the seventh of nine evenly spaced wells. The plot shows the energy eigenvalues as a function of the defect well position b_7 with $\beta = 10$ for all wells, so the results for $b_7 = 7$ correspond exactly to the results for $\beta = 10$ in Fig. 3 as

well as for $N = 9$ in Fig. 1. The Bloch bands for the infinitely periodic system with $\beta = 10$ are shown in Fig. 8 for reference. Note that the plot covers a domain $5 < b_7 < 9$ in order to illustrate what happens if the defect well is displaced beyond one of its neighboring wells. Extending the domain farther does not produce any qualitatively different results unless the defect location approaches one of the hard walls, a case which will be discussed later.

Figure 8 shows that, like the strength defect examined previously, the position defect can alter the energy spectrum of the system, but the character of the alteration is different from the case of the strength defect. The position defect generally causes the positive energy levels to oscillate as b_7 is varied. All positive energy levels are thus affected, even the ISW levels, because no eigenfunction can have a node at all possible locations of the defect well. The amplitude of each level's oscillation is relatively constant in the range $6 < b_7 < 8$ but as the defect moves past the neighboring well the amplitude of the oscillation may change noticeably, either increasing or decreasing. The oscillation of the levels mostly produces a modulation of the size of the energy bands, however for the lowest positive energy band the top level shifts into the gap above this band, and the bottom levels shifts into the gap below this band, as the defect moves past the neighboring well. For some values of b_7 the lowest positive energy level ($n = 10$) is pushed back upward into the lowest energy band after an avoided crossing with the $n = 9$ level that has shifted upward to become positive, but the $n = 9$ level essentially takes the place of the $n = 10$ level in the gap below the first positive energy band. We do not see any level move all the way across a band gap as we saw in the case of a strength defect.

The negative energy levels are clustered near $E = -25$ when $b_7 \approx 7$. As the defect well moves closer to one of its neighboring wells the $n = 1$ level moves toward lower energies while the $n = 9$ level moves upward, becoming positive when the defect is very close to the neighboring well and the two wells begin to merge into a single well with a doubled strength. When the defect well lies at the location of a neighboring well we see eight negative energy levels: seven levels clustered near the usual value of $E = -25$ and one with $E \approx -100$ (the bound state energy for a single delta well with $\beta = 20$). The merger of the two wells reduces the total number of wells and thus the number of negative-energy states, but since the merged well has twice the strength of the other wells one of the negative-energy states has a much lower energy than the others. As the defect moves past the neighboring well the $n = 1$ and $n = 9$ levels move back toward $E = -25$, approaching closest when the defect

well is midway between two other wells (e.g. at $b_7 = 5.5$ or 8.5). However, these levels never return to the compact cluster near $E = -25$ and as the defect approaches the next well ($b_7 \approx 5$ or 9) these levels move back to the values they had for $b_7 \approx 6$ or 8.

Figure 9 shows a detail from Fig. 8 to illustrate the behavior of the cluster of negative energy states near $E = -25$. The eigenvalue curves display a series of avoided crossings near $b_7 = 5.5$, 7, and 8.5 when the $n = 1$ and $n = 9$ levels approach the cluster. The $n = 1$ and $n = 9$ levels are visible in the Figure for $b_7 \approx 7$. The avoided crossings produce a noticeable shift in the levels, but away from these avoided crossings the levels in this cluster remain approximately constant as b_7 is varied.

Figure 10 shows selected (unnormalized) energy eigenfunctions for our model system with a position defect with $b_7 = 5.5$ (so there is an "extra" well at $x = 5.5$ and a vacancy at $x = 7$). For this value of b_7 the $n = 1$ level is well below, and the $n = 9$ level is well above, the cluster of negative energies at $E = -25$. The eigenfunctions for these two states are strongly peaked at the location of the defect well at $x = 5.5$, as seen for the $n = 1$ state in Fig. 10. Similarly, the $n = 10$ level has moved into the gap below the first positive energy band and the $n = 19$ level has moved into the gap above the first positive energy band. The eigenfunctions for these states are peaked at the location of the vacancy at $x = 7$, as seen for the $n = 10$ state in Fig. 10. Thus we see that the states most strongly affected by changing b_7 are either peaked at the location of the defect (similar to what we saw for strength defects) or at the location of the vacancy. The eigenfunctions for other states in the negative energy band and the first positive energy band show a tendency to have their probability concentrated on one side or the other of the defect (e.g. the $n = 2$ and $n = 11$ states in Fig. 10). This tendency is much less noticeable for states in the higher energy bands. Note that in general the eigenfunctions do not have well-defined symmetry (except when $b_7 = 7$) since the symmetry of the potential energy function is broken by the position defect. Although it is difficult to see in the plots, the wave functions do still have a number of nodes equal to $n - 1$.

The behavior shown for a position defect at the seventh well is typical. Introducing a position defect at a different well location produces qualitatively similar results, with two exceptions. If the defect is introduced at the fifth well, then the plot of energy eigenvalues versus b_5 is perfectly symmetric about $b_5 = 5$. This symmetry arises because, for example, the system with $b_5 = 5.2$ is identical to the system with $b_5 = 4.8$ reflected about the center

of the well at $x = 5$. The other exception is if the defect well approaches one of the walls of the ISW. In that case, as the defect well approaches the location of the wall the $n = 1$ state will maintain an energy near $E = -25$ rather than dropping to lower energies as in the case examined above, but the energy of the $n = 9$ state will still become positive. Although an isolated delta well always supports a negative-energy state, a delta well near a boundary may not support a negative-energy state. As the delta well reaches the boundary the well effectively disappears from the system. The system will then have only eight delta wells, all with the same strength, so it will support eight negative energy states all with similar energies, much like the case of the strength defect with $\beta_7 = 0$.

VI. CONCLUSION

We have shown that a simple system consisting of an infinite square well containing N periodically spaced delta wells exhibits the formation of band structure in the energy spectrum. The energy eigenvalues for this system can be easily computed and the energy spectrum shows level splitting with the formation of well-defined energy bands separated by band gaps as N is increased. In addition, we have investigated two types of defects in this system: strength defects and position defects. Strength defects, in which the strength of one of the delta wells is altered, can lead to energy levels moving out of the usual energy bands and into, or even across, the band gaps. On the other hand position defects, in which the position of one of the delta wells is altered, produce a modulation in the size of the energy bands and gaps and, if the defect well moves past one of its neighboring wells, can result in some levels moving into a gap region. The energy eigenfunctions of those states whose energies are most strongly altered by the defect are found to be peaked at the location of the defect, or the location of the vacancy in the case of a position defect, while there is some tendency, most strongly pronounced for lower energy states, for other eigenfunctions to be concentrated on one side or the other of the defect.

The investigation of this model requires only standard techniques usually learned in introductory quantum mechanics: finding the general form of the energy eigenfunctions and then using boundary conditions to determine the allowed energy eigenvalues. Moreover, the computation of the eigenvalues requires nothing more difficult than the numerical solution of a transcendental equation. Thus, this simple model can provide an effective introduc-

tion to important concepts related to periodic quantum systems and can help to bridge the gap between basic quantum mechanics and more abstract approaches like Bloch's theorem. Furthermore, this model allows for the direct investigation of defects and can be used to illustrate how impurities and dislocations can alter the energy spectrum of a periodic quantum system.

The computations required to investigate this system are relatively easy to perform. Code notebooks for all of the computations shown, using the open-source *Maxima* computer algebra system, are available at the author's website . We encourage readers to obtain the code and explore this simple model themselves. Although we have tried to provide a general overview of the behavior of this model, there are many more behaviors that can be explored. For example, one could investigate the role of the delta well strength (β) in determining the results of a position defect, explore defects in which both the position and strength of one of the delta wells is changed, or use alternating values of β to simulate a diatomic crystal (like NaCl). In addition, this quantum model is analogous to a simple acoustical system of a pipe with closed ends and divided into segments by baffles or washers. Experimental investigations of this acoustical system have shown the formation of band structure,[2,3] but our quantum model could be used to guide the exploration of defects in these acoustical systems.[37]

---

[1] Robert Eisberg and Robert Resnick. *Quantum physics of atoms, molecules, solids, nuclei, and particles*, (Wiley, New York, 2nd edition, 1985), pp. 445–450.

[2] Christopher Carr and Roger Yu. "Sonic band structure and localized modes in a density-modulated system: Experiment and theory," Am. J. Phys. **70**, 1154–1156 (2002).

[3] Marissa D'Onofrio, Mitchell Crum, Shawn A Hilbert, Herman Batelaan, Timothy Canalichio, and Tyler Bull. "An acoustic analog for a quantum mechanical level-splitting route to band formation," Am. J. Phys. **84**, 841–847 (2016).

[4] Parker Roberts, Alexandria Skinner, Tadan Cobb, Scott Carr, and Shawn A Hilbert. "A classical analogy for quantum band formation," Am. J. Phys. **86** 609–615 (2018).

[5] David J Griffiths. *Introduction to Quantum Mechanics*, (Pearson, Upper Saddle River, NJ, 2nd edition, 2005), pp. 224–229.

[6] Neil Ashcroft and N. David Mermin. *Solid state physics*, (Holt, Reinhart and Winston, New York, 1976), pp. 131–150.

[7] R de L Kronig and William George Penney. "Quantum mechanics of electrons in crystal lattices," Proc. R. Soc. Lond. A, **130** 499–513 (1931).

[8] AA Bahurmuz and PD Loly. "Model bandstructure calculations," Am. J. Phys. **49** 675–680 (1981).

[9] RL Pavelich and Frank Marsiglio. "The Kronig-Penney model extended to arbitrary potentials via numerical matrix mechanics," Am. J. Phys. **83** 773–781 (2015).

[10] David J Griffiths and Carl A Steinke. "Waves in locally periodic media," Am. J. Phys. **69** 137–154 (2001).

[11] Felipe Le Vot, Juan J Meléndez, and Santos B Yuste. "Numerical matrix method for quantum periodic potentials," Am. J. Phys. **84** 426–433 (2016).

[12] Dae-Yup Song. "Energy splitting in a finite periodic multiple-well potential," Eur. J. Phys. **38** 055401 (2017).

[13] DWL Sprung, JD Sigetich, Hua Wu, and J Martorell. "Bound states of a finite periodic potential," Am. J. Phys. **68** 715–722 (2000).

[14] David Kiang. "Multiple scattering by a dirac comb," Am. J. Phys. **42** 785–787 (1974).

[15] Hai-Woong Lee, Adam Zysnarski, and Phillip Kerr. "One-dimensional scattering by a locally periodic potential," Am. J. Phys. **57** 729–734 (1989).

[16] David J Griffiths and Nicholas F Taussig. "Scattering from a locally periodic potential," Am. J. Phys. **60** 883–888 (1992).

[17] DWL Sprung, Hua Wu, and J Martorell. "Scattering by a finite periodic potential," Am. J. Phys. **61** 1118–1124 (1993).

[18] Raina J Olsen and Giovanni Vignale. "The quantum mechanics of electric conduction in crystals," Am. J. Phys. **78** 954–960 (2010).

[19] Braulio Gutiérrez-Medina. "Wave transmission through periodic, quasiperiodic, and random one-dimensional finite lattices," Am. J. Phys. **81** 104–111 (2013).

[20] PR Berman. "Transmission resonances and Bloch states for a periodic array of delta function potentials," Am. J. Phys. **81** 190–201 (2013).

[21] ID Johnston and D Segal. "Electrons in a crystal lattice: A simple computer model," Am. J. Phys. **60** 600–607 (1992).

[22] Robert Gilmore. *Elementary Quantum Mechanics in One Dimension*, (The Johns Hopkins University Press, Baltimore, MD, 2004), pp. 167–211.

[23] Mario Belloni and RW Robinett. "The infinite well and Dirac delta function potentials as pedagogical, mathematical and physical models in quantum mechanics," Phys. Rep. **540** 25–122 (2014).

[24] Ernesto Cota, Jorge Flores, and Guillermo Monsivais. "A simple way to understand the origin of the electron band structure," Am. J. Phys. **56** 366–372 (1988).

[25] David C. Johnston "Attractive Kronig-Penney Band Structures and Wave Functions," arXiv:1905.12084v2 (2019).

[26] See Ref. 5, pp. 70–73.

[27] See Ref. 22, p. 15–18.

[28] M Belloni, MA Doncheski, and Richard Wallace Robinett. "Zero-curvature solutions of the one-dimensional Schrödinger equation," Phys. Scr. **72** 122–126 (2005).

[29] LP Gilbert, M Belloni, MA Doncheski, and Richard Wallace Robinett. "Piecewise zero-curvature energy eigenfunctions in one dimension," Eur. J. Phys. **27** 1331–1339, (2006).

[30] LP Gilbert, M Belloni, MA Doncheski, and Richard Wallace Robinett. "Playing quantum physics Jeopardy with zero-energy eigenstates," Am. J. Phys. **74** 1035–1036 (2006).

[31] Zafar Ahmed and Swayam Kesari. "The simplest model of the zero-curvature eigenstate," Eur. J. Phys. **35** 018002 (2013).

[32] Urbano Oseguera. "Effect of infinite discontinuities on the motion of a particle in one dimension," Eur. J. Phys. **11** 35–38 (1990).

[33] See Ref. 5, p. 73.

[34] However, a given ISW eigenvalue does not correspond to the *same* eigenstate for different values of N. For example, the $n = 1$ state for $N = 0$ has the same energy as the $n = 3$ state for $N = 2$.

[35] See Ref. 5, pp. 73–76.

[36] We chose to place the defect at well seven of nine primarily because it produces typical results, but we hope that some readers will also appreciate the nod to Star Trek. After all, by moving out of its periodic position the defect well is no longer assimilated into the collective.

[37] In fact, our study of this quantum model was inspired by a preliminary study of defects in an acoustical system conducted by Shawn Hilbert, Scott Carr, and Raphael Paolo Francisco.

Appendix A: Figures

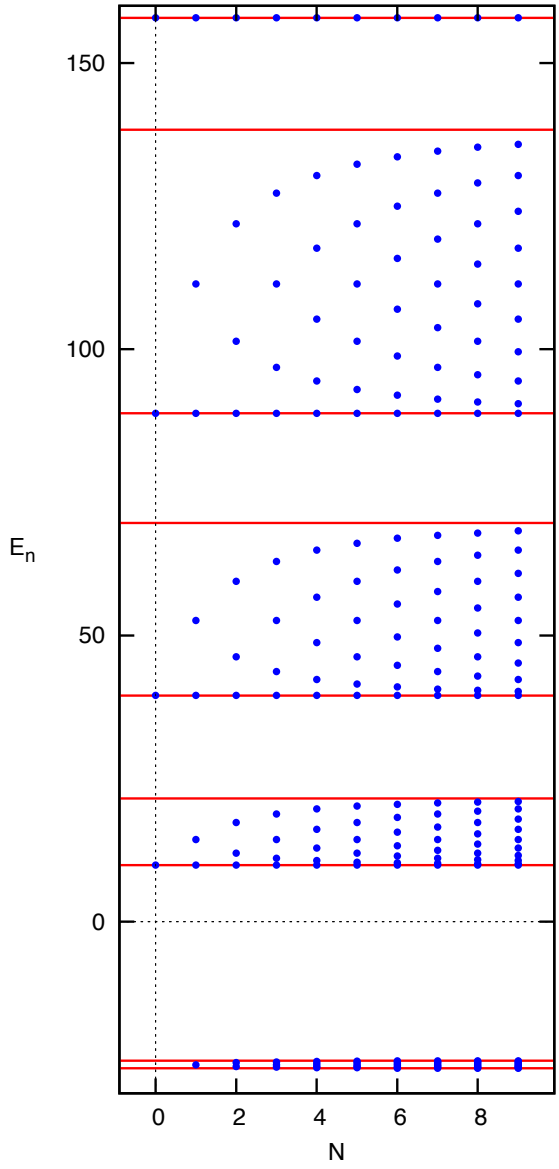

FIG. 1. Lowest $4N + 4$ energy eigenvalues (E_n) as a function of the number (N) of evenly spaced delta wells all with $\beta = 10$. The solid (red) curves are the boundaries of the Bloch bands.

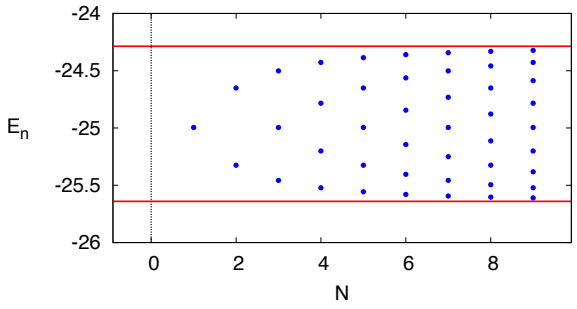

FIG. 2. Detail of negative energy eigenvalues (E_n) as a function of the number (N) of evenly spaced delta wells all with $\beta = 10$. The solid (red) curves are the boundaries of the Bloch bands.

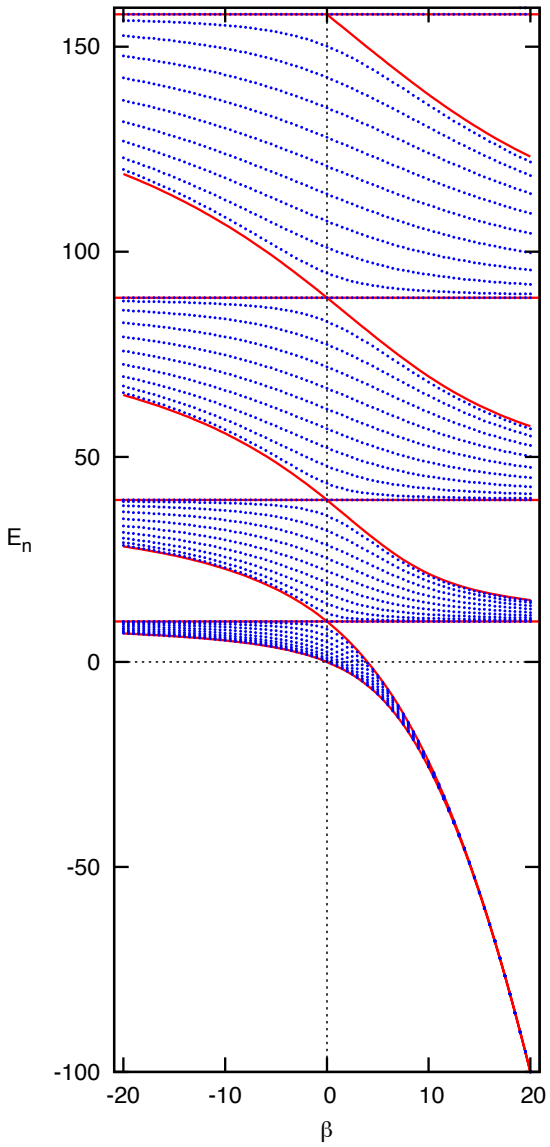

FIG. 3. Lowest 40 energy eigenvalues (E_n) as a function of β with $N = 9$ evenly spaced delta wells. The solid (red) curves are the boundaries of the Bloch bands.

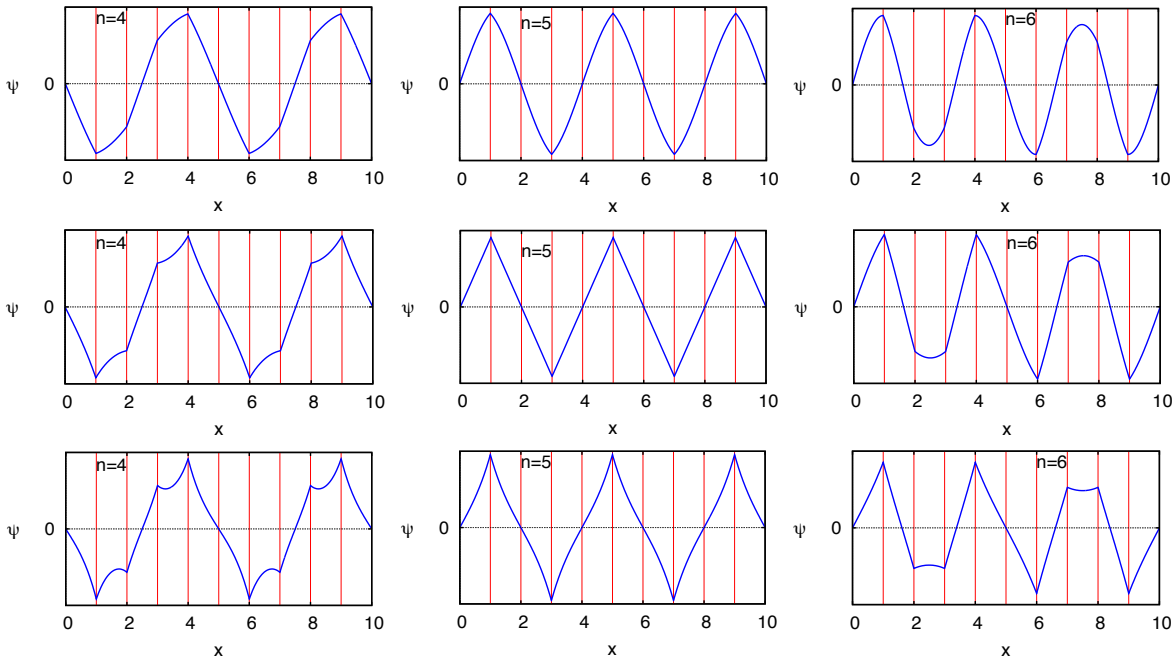

FIG. 4. Unnormalized energy eigenfunctions ($n = 4$, 5, and 6) with 9 evenly spaced delta wells and three different values of β. For the top row, $\beta = 1$ ($E_4 \approx 0.479, E_5 \approx 1.36, E_6 \approx 2.43$). For the middle row $\beta = 2$ ($E_4 \approx -0.852, E_5 = 0, E_6 \approx 1.03$). For the bottom row $\beta = 3$ ($E_4 \approx -2.46, E_5 \approx -1.66, E_6 \approx -0.704$). The thin (red) horizontal lines show the locations of the delta wells.

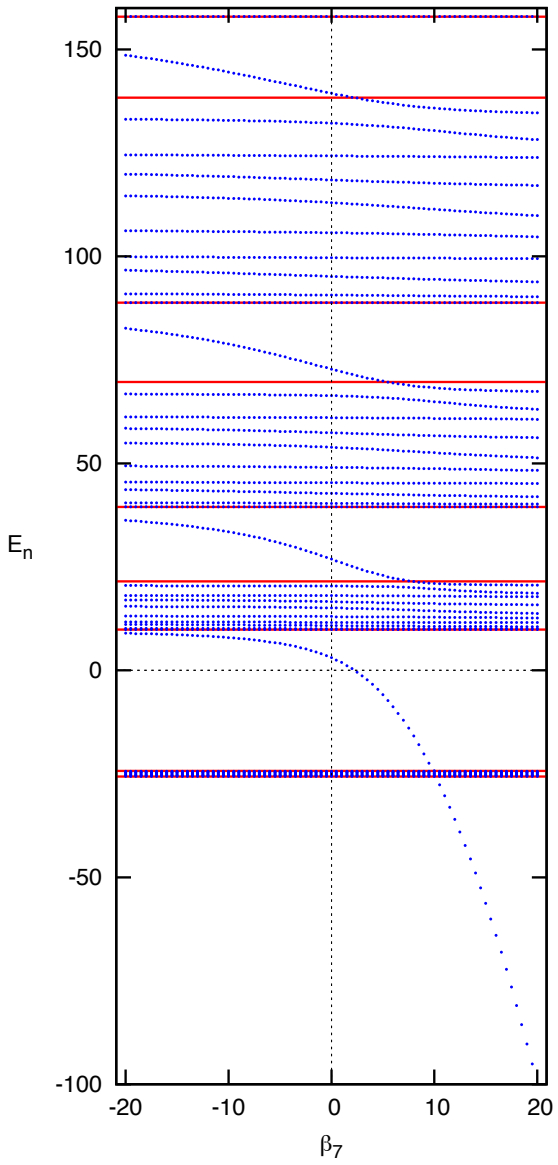

FIG. 5. Lowest 40 energy eigenvalues (E_n) for $N = 9$ evenly spaced delta wells with $\beta = 10$ except for a strength defect in the seventh well. Eigenvalues are shown as a function of the defect strength (β_7). The solid (red) curves are the boundaries of the Bloch bands.

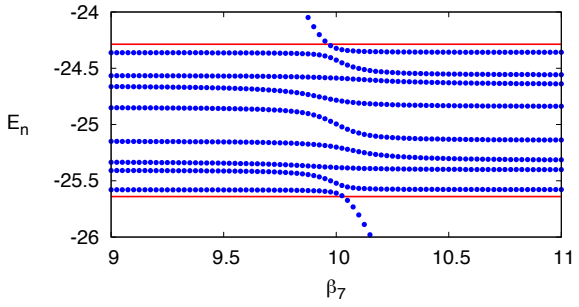

FIG. 6. Detail of negative energy eigenvalues (E_n) as a function of β_7 from Figure 5. The solid (red) curves are the boundaries of the Bloch bands.

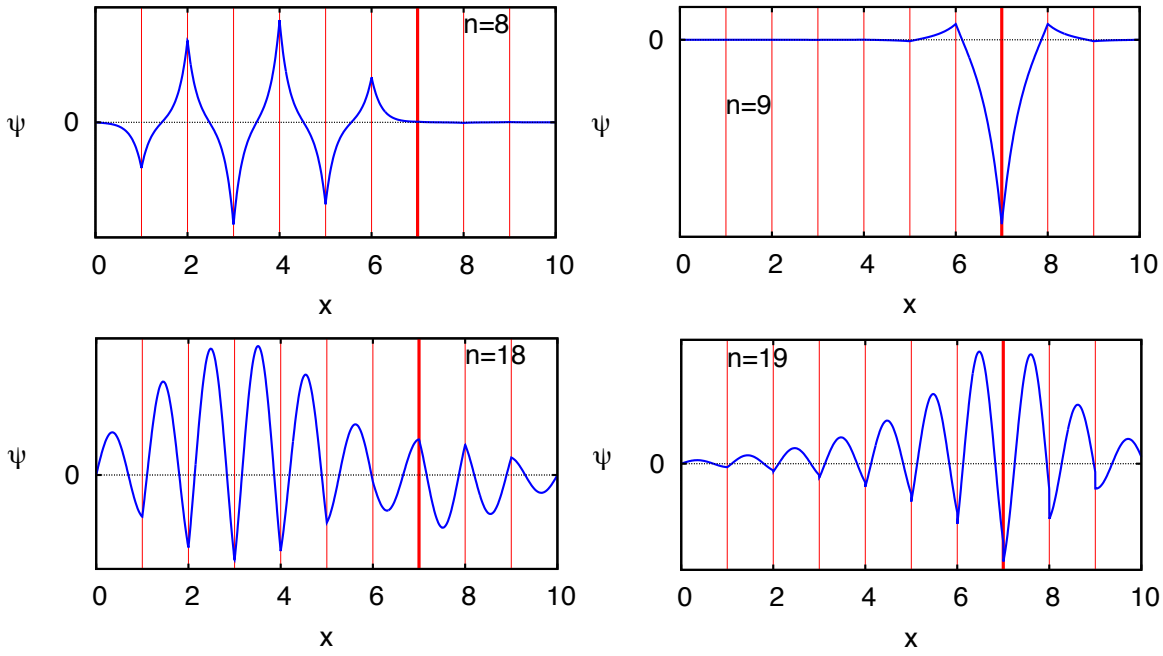

FIG. 7. Unnormalized energy eigenstate wave functions for 9 evenly spaced delta wells all with $\beta = 10$ except for a strength defect of $\beta_7 = 5$ in the seventh well. The states shown are: $n = 8$ ($E \approx -24.4$), $n = 9$ ($E \approx -5.88$), $n = 18$ ($E \approx 20.2$), and $n = 19$ ($E \approx 22.9$). The thin (red) horizontal lines show the locations of the delta wells with the thicker line indicating the location of the strength defect.

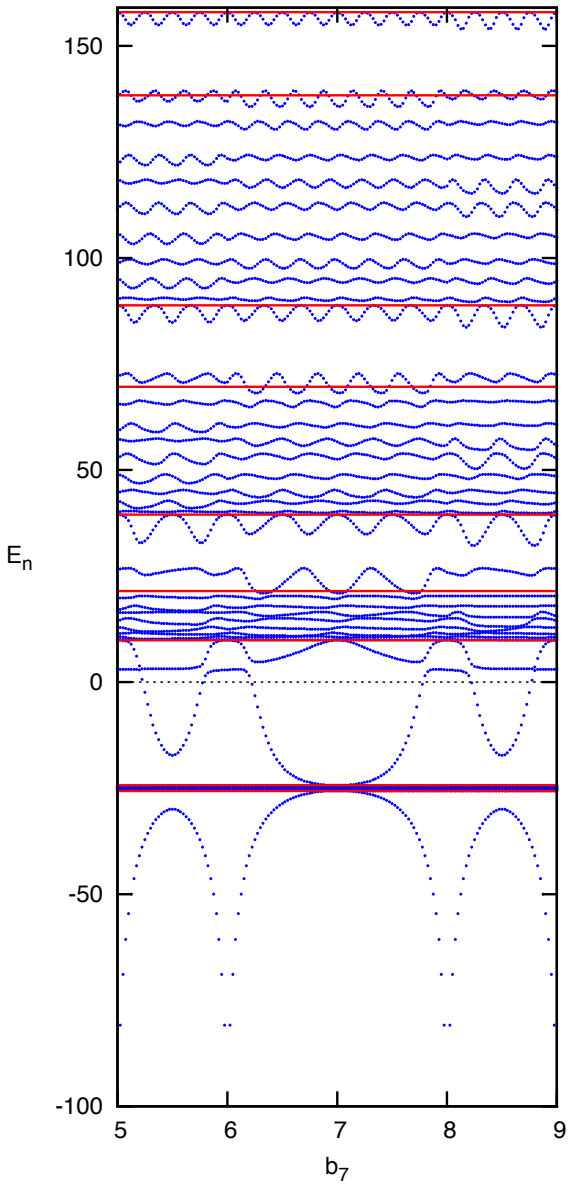

FIG. 8. Lowest 40 energy eigenvalues (E_n) for $N = 9$ delta wells with $\beta = 10$ and evenly spaced except for a position defect in the seventh well. Eigenvalues are shown as a function of the defect position (b_7). The solid (red) curves are the boundaries of the Bloch bands.

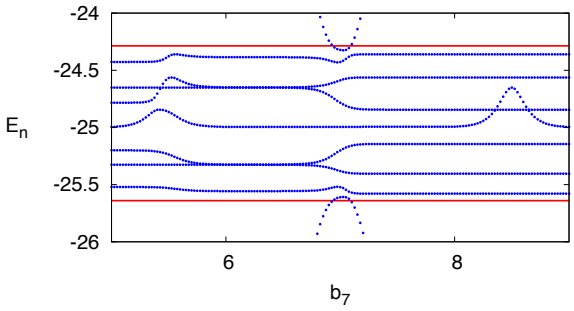

FIG. 9. Detail of negative energy eigenvalues (E_n) as a function of b_7 from Figure 8. The solid (red) curves are the boundaries of the Bloch bands.

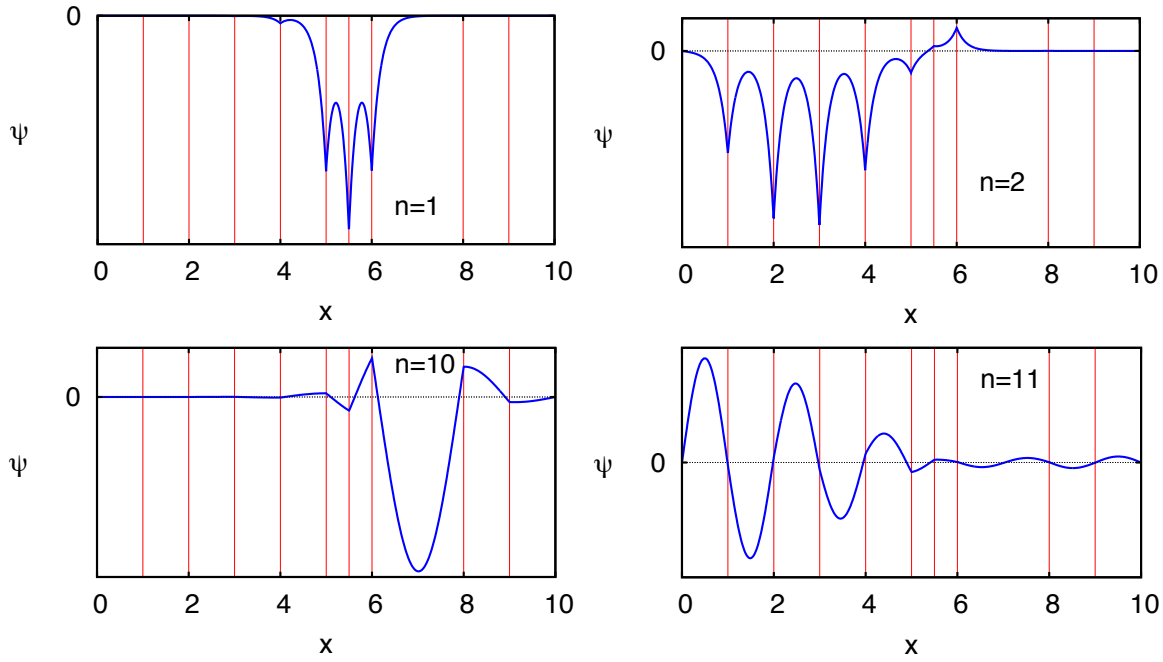

FIG. 10. Unnormalized energy eigenfunctions for 9 delta wells with $\beta = 10$ and evenly spaced except for a position defect in the seventh well with $b_7 = 5.5$. The states shown are: $n = 1$ ($E \approx -29.9$), $n = 2$ ($E \approx -25.5$), $n = 10$ ($E \approx 3.13$), and $n = 11$ ($E \approx 10.0$). The thin (red) horizontal lines show the locations of the delta wells.